JOURNAL BEARING DESIGN TYPES AND THEIR APPLICATIONS TO TURBOMACHINERY

by
Dana J. Salamone
Chief Engineer
Centritech Corporation
Houston, Texas

Dana J. Salamone received his B.S. in Mechanical Engineering in 1974 and his M.S. in Applied Mechanics in 1977, both from the University of Virginia. He also earned an M.B.A. from Houston Baptist University in 1984.

He spent the first three years of his engineering career at Babcock and Wilcox, in Lynchburg, Virginia, where he was responsible for seismic structural design, stress analysis, and rotor dynamics analysis. He spent two years as a Project Engineer in the Compressor Division of Allis-Chalmers Corporation in Milwaukee, Wisconsin. He was responsible for rotor dynamics analysis of multistage centrifugal compressor and 3-D finite element stress analysis of horizontally-split fabricated casings.

Mr. Salamone became Chief Engineer for Centritech Corporation in Houston, Texas, in 1979. He is a Bearing Designer and Consultant to the utility, petroleum and chemical industries for the solution of turbomachinery vibration problems.

He has several publications on rotor dynamics with ASME, the Turbomachinery Symposium and the Vibration Institute.

Mr. Salamone is a member of ASME, ASLE, the Vibration Institute, and the National Society of Professional Engineers. He is an associate member of Sigma Xi and a registered professional engineer in the State of Texas.

ABSTRACT

A review of several different types of hydrodynamic journal bearings that are commonly found in turbomachinery is presented. Emphasis is placed on the key geometric design parameters of each type. The discussion covers plain journal, axial groove, pressure dam, offset split, lemon bore, multilobe and titling-pad bearings.

The application of the critical speed map and some basic non-dimensional bearing parameters as tools for preliminary bearing selection and comparison are discussed. These tools are applied to two case studies, which demonstrate the proper application of different bearing designs to industrial turbomachinery.

INTRODUCTION

Industrial turbomachinery, such as steam turbines, gas compressors, pumps and motors, contain a variety of different types of hydrodynamic journal bearings. The types of bearings most commonly found in turbomachinery include:

- plain cylindrical
- axial grove
- pressure dam
- lemon bore
- offset pivot
- three-lobe
- four-lobe
- tilting-pad

The reason for such a large selection of bearings is that each of these types has unique operational characteristics that render it more suitable for one application than another [1,2,3,4,5].

The fundamental geometric parameters for all journal bearings are diameter, pad arc angle, length-to-diameter ratio, and running clearance. For the bearing types consisting of multiple pads, there are also variation in the number of pads, preload, pad pivot offset angle, and orientation of the bearing (on or between pads). In addition to the geometric parameters, there are several important operating parameters. The key operating parameters are oil viscosity, oil density, rotating speed, gravity load at the bearing, and applied external loads. Volute loads in pumps and mesh loads in gear boxes are examples of external loads.

The plain journal bearing, shown in Figure 1, is the most basic hydrodynamic journal bearing. As the name implies, this bearing has a plain cylindrical bore. A shaft rotating in a plain journal bearing is illustrated in Figure 2. The eccentric rotating shaft will develop an oil film pressure profile, as shown in the figure. If this pressure profile is integrated around the bearing, a net resisting force to oppose the imposed load, W, results. The position at which there is a balance between the imposed load and the hydrodynamic force is called the equilibrium position. The shaft eccentricity, e, is the distance between the displaced shaft at equilibrium and the bearing center. In horizontal turbomachinery, the imposed bearing loads are due to the gravitational weight of the rotor. In addition to the gravity load, there can be external bearing loads as previously mentioned.

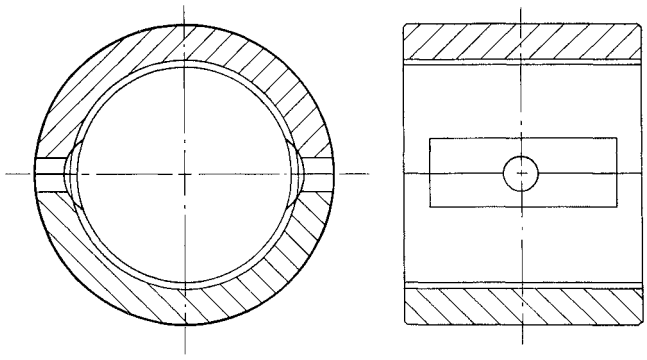

Figure 1. Plain Journal Bearing.

The four axial groove journal bearing [6,7], illustrated in Figure 3, is another variation of a plain journal bearing. This design incorporates four axial grooves, 90° apart, which are normally located at 45 degrees from the vertical axis. This

design is more stable than the plain journal bearing for some applications [6].

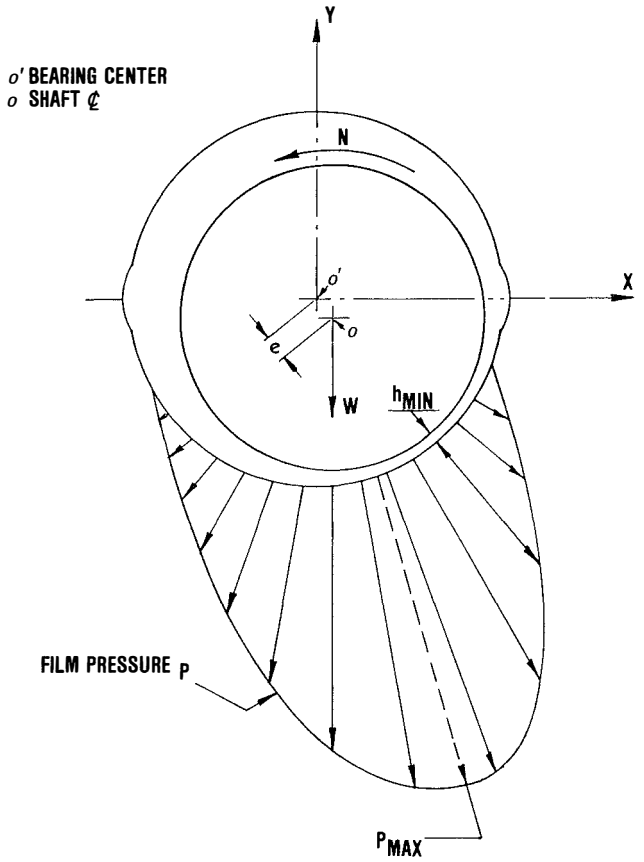

Figure 2. Hydrodynamic Bearing Pressure Profile.

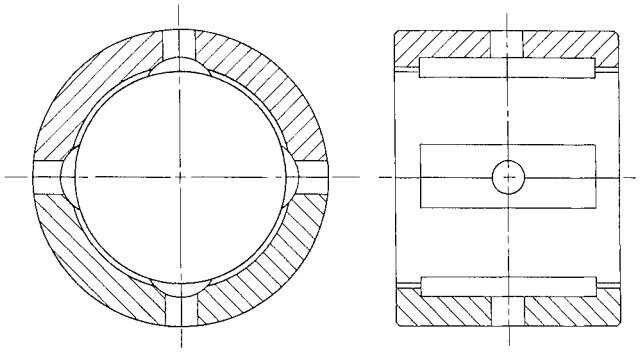

Figure 3. Four-Axial Groove Journal Bearing.

The pressure dam journal bearing [8,9,10] is shown in Figure 4. This bearing is also similar to the plain bearing except that it incorporates a circumferential relief scallop, with depth, d, in the top half. The relief ends abruptly in a step at some angle θ_s from the horizontal split line, as shown in the figure. The pressure differential before and after the step creates a net loading that forces the journal down into the bottom half of the bearing and can significantly increase stability [8]. Another variation of this bearing incorporates a circumferential relief groove in the bottom half. This groove reduces the unit area of the bearing and therefore increases the bearing unit loading.

The bearing designs described could be classified as variations of the plain journal bearing because the babbitt bore is

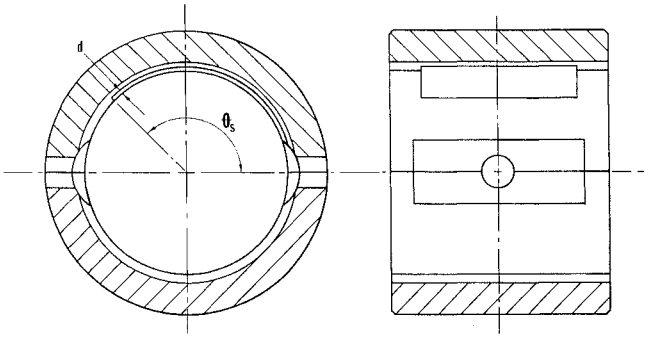

Figure 4. Pressure Dam Journal Bearing.

concentric with the journal, when the journal is centered in the bearing. The rest of the bearing designs to be discussed are more complex because they consist of two bores (the bearing set bore and the pad machines bore). The combination of these two bores determines a non-dimensional parameter known as preload. A bearing pad with a machined bore radius R_p centered at O_p, and a set bore radius R_b, centered at the true bearing center O_b is shown in Figure 5. If O_p is coincident with O_b, then $R_p = R_b$ and the preload is zero. In this case, if the journal is centered in the bearing, the pad arc will be concentric with the journal surface. If the pad bore is larger than the set bore, the centers of curvature will be offset, as shown in the figure. The set bore radius is the distance from the true bearing center to the pad surface at the point of minimum clearance from the centered shaft. The set bore radius can also be described as the radius of the largest mandrel that could be inserted into the assembled bearing. If the pad machined bore is held at a fixed value, the preload is increased by moving the pad radially inward toward the shaft. The extreme value of preload results when the pad contacts the shaft. In this condition, the set clearance is zero and the preload is unity. Preload forces the oil to converge at each pad because of the reduced clearance at the mid point of the pad, where the clearance-sized mandrel would make contact. The result is an oil wedge effect.

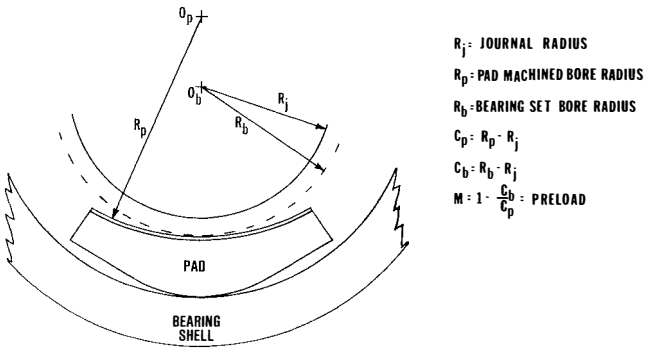

Figure 5. Bearing Preload.

The lemon bore (elliptical) bearing [11] is a two-pad-fixed geometry bearing which is preloaded in the vertical direction, as shown in Figure 6. This bearing can be manufactured by inserting a shim in the split line before boring. When the shim is removed, the vertical clearance will be less than the horizontal clearance. Note that the centers of curvature of the top and bottom halves are not coincident with the true bearing center in the figure.

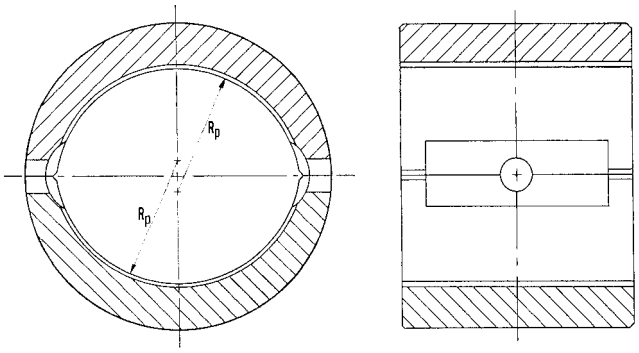

Figure 6. Lemon Bore Journal Bearing.

The offset split bearing [11] is shown in Figure 7. This bearing is preloaded in the horizontal direction. It is manufactured by offsetting the halves before finish boring such that, when the halves are matched, the pad centers will be horizontally offset. In this bearing, the horizontal clearance is smaller than the vertical clearance. The vertical clearance equals the pad machined clearance. The horizontal diametral clearance is equal to the pad machined diametral clearance, minus twice the radial offset.

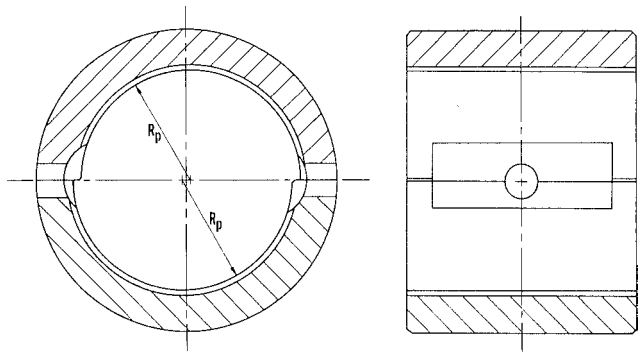

Figure 7. Offset Split Journal Bearing.

Three-lobe (Figure 8) and four-lobe (Figure 9) bearings belong to a class of bearing called multilobe bearings [11,12,13,14,15,16]. These bearings are similar in concept to the lemon bore bearings (i.e., there is a separate pad machined bore and bearing set bore). Note that the centers of pad arc for each of the lobes form a circle, referred to as a preload circle. Therefore, a wide range of preloads is possible by changing the pad and set bores.

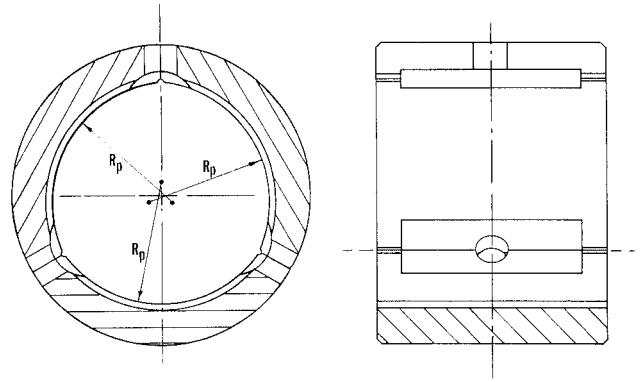

Figure 8. Three-Lobe Journal Bearing.

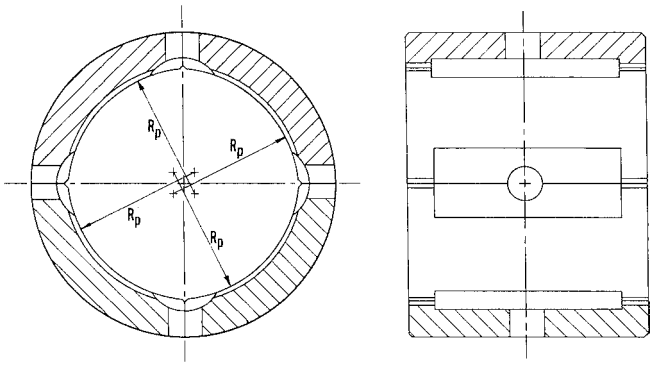

Figure 9. Four-Lobe Journal Bearing.

Up to this point, the discussion has addressed several styles of fixed geometry, or fixed pad, bearings. Each of these bearings has specific advantages in different applications, but they all have a characteristic called cross-coupled stiffness, which creates an out-of-phase force to the displacement and couples the equations of motion for the lateral degrees of freedom. Under certain conditions, this cross-coupling can cause the bearing to be unstable and an oil whirl will result.

The tilting-pad journal bearing [17,18,19,20,21,22,23] consists of several individual journal pads which can pivot in the bore of a retainer. The tilting pad is like a multilobe bearing with pivoting lobes, or pads. The same concept of preload applies to the tilting-pad bearing. The pads have a machined bore and these pads can be set into a retainer to achieve a particular bearing set bore. The primary advantage of this design is that each pad can pivot independently to develop its own pressure profile. This independent pivoting feature significantly reduces the cross-coupled stiffness. In fact, if pad pitch inertia is neglected and the bearing is symmetric about the vertical axis, the cross-coupled stiffness terms are eliminated [17]. The number of pads utilized in the tilting-pad bearing can be three, four, five, or seven. However, the most common tilting-pad bearing arrangements have four or five pads. The rocker pivot and the spherical pivot arrangements are illustrated in Figures 10 and 11, respectively. The rocker design has a line-contact pivot between the pad and the bearing retainer. As the name implies, the spherical design has a semispherical surface-contact pivot. Both of these designs allow the pads to pitch in the conventional manner. However, the spherical design has the additional ability to accommodate shaft misalignment.

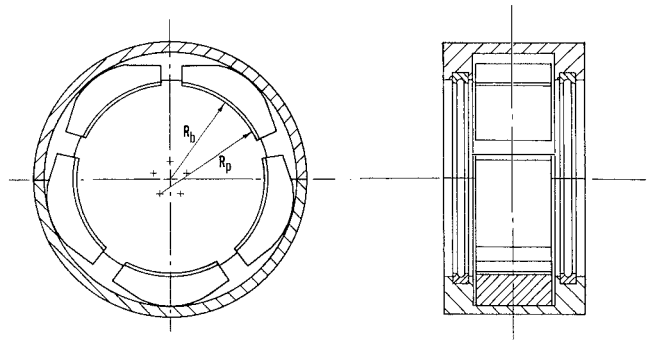

Figure 10. Rocker Pivot Tilting-Pad Journal Bearing.

KEY DESIGN PARAMETERS

The discussion of preload brought out the distinction between two different bearing bores. These are pad machined

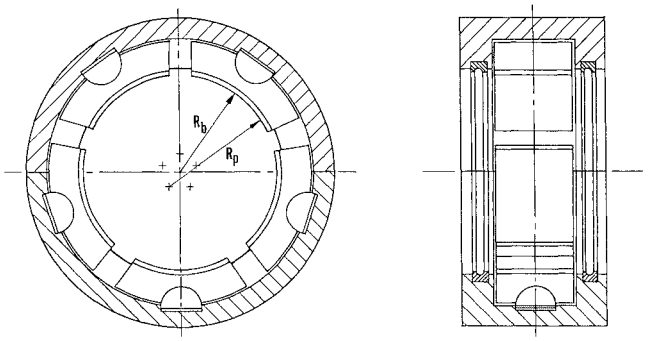

Figure 11. Spherical Pivot Tilting-Pad Journal Bearing.

bore and bearing set bore. Note that the plain journal, axial groove and pressure dam bearings have only one bore (the set bore is the same as the pad bore). The difference between the pad machined bore radius and the journal radius is the pad machined clearance. The difference between the bearing set bore radius and journal radius is the bearing set clearance. The set clearance is the same as the running clearance, which is often specified as a clearance ratio of mils (milli-inches) per inch of journal diameter. Some typical values of clearance ratio are between 1.5 to 2.0 mils/in. Obviously, there are some applications where these values do not apply. The manufacturer will specify the recommended clearances for the particular bearing application.

Slenderness ratio is also referred to as L/D ratio. This is the ratio of the bearing length to the shaft diameter. This ratio typically varies between 0.2 and 1.0. However, some plain journal bearings have slenderness ratios above 1.0. The bearing length affects the stiffness and damping characteristics of the bearing. In the selection of a bearing length, one must consider the bearing unit loading. The unit load is the bearing load divided by the product of the bearing length and the shaft diameter; therefore, the units are psi. Typical values of unit loading are between 150 and 250 psi.

UNDAMPED CRITICAL SPEED MAP

An example of a typical critical speed map for a rotor supported between two bearings is depicted in Figure 12. This is a plot of the undamped critical speeds, as a function of the bearing stiffness. The map illustrates the effect of bearing stiffness on the rotor critical speeds. In the flexible bearing region, the shaft is stiff, relative to the bearings. Therefore, bearing stiffness can significantly affect the critical speeds because the criticals increase as the bearing stiffness is increased. In the stiff bearing region, the critical speeds become asymptotic to an upper limit as which the bearings are rigid relative to the rotor shaft. Hence, they are called the rigid bearing critical speeds.

In order to control shaft dynamics, a designer must select a bearing with stiffness and damping qualities that are compatible with the rotor. If the bearings are too stiff, the effectiveness of the bearing damping will be limited, regardless of the theoretical damping coefficient value. Three undamped critical speed curves are shown on the map in Figure 12. These modes are the first three natural frequencies of the rotor bearing system.

The combination of different bearing types, geometries, and imposed operating conditions provides a broad selection of different stiffness and damping properties. Therefore, some bearings will be better than others for a particular application. When the actual bearing stiffness is plotted on the critical speed map, the intersections indicate the undamped critical

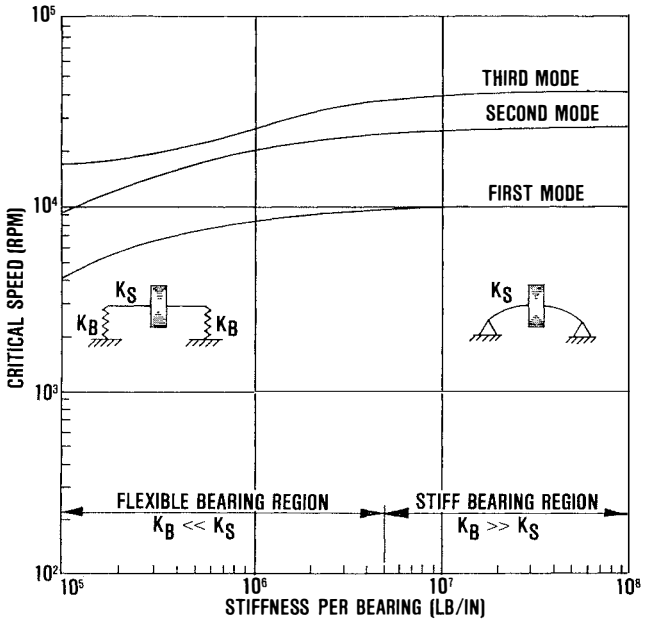

Figure 12. Typical Undamped Critical Speed Map.

speeds. It should be noted that the stiffness of an actual hydrodynamic bearing is a complex quantity:

$$K_c = K_{uv} + i\omega c_{uv} \quad (1)$$

where: the subscripts u and v denote the principal lateral directions, x or y.

The real term K_{uv} is the stiffness coefficient. The imaginary term ωc_{uv} is the product of the damping coefficient and the angular speed. Therefore, the undamped critical speeds from the map are only an approximation of the actual damped critical speeds.

BEARING STIFFNESS AND DAMPING RELATIONSHIPS

In addition to the critical speed map, the designer can use some basic non-dimensional quantities to compare different bearing designs. The relationships presented here were developed by Barrett, Gunter and Allaire[24], based on the single-mass rotor. The single-mass rotor on damped, elastic bearings is illustrated in Figure 13. This model, commonly referred to as the Jeffcott model [25], has been frequently used by researchers to investigate rotor dynamic behavior. These basic single-mass rotor relationships can then be applied as approximations to determine complex industrial rotor characteristics provided that the major masses of the complex rotor, such as wheels, are mounted between the bearings and provided there is a relatively symmetric mass distribution.

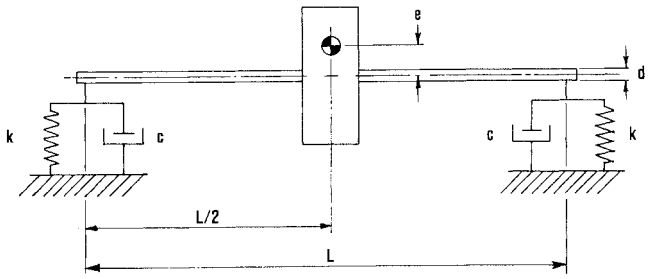

Figure 13. Single-Mass Rotor.

The effective shaft stiffness can be calculated from the rigid bearing critical speed and the modal mass of the rotor by using the equation:

$$K_s = \omega^2_{cr} M_m$$

where ω_{cr} = the rigid bearing critical speed (rad/sec)
K_s = the effective shaft stiffness (lb/in)
M_m = the rotor modal mass on rigid supports (lb-sec^2/in)
= approximately $W_{rotor}/2g$

The total critical bearing damping can also be calculated as:

$$C_{cr} = 2\ M_m \omega_{cr}$$

The stiffness ratio [24] is the total bearing stiffness divided by the rotor stiffness, or:

$$\bar{K} = (K_{b1} + K_{b2})/K_s$$

where K_{b1} and K_{b2} are the stiffness for each of the bearings. It is recommended that this ratio be limited to six or less.

The damping ratio [24] is the total actual bearing damping divided by the total critical damping, or:

$$\xi_{act} = (C_{b1} + C_{b2})/C_{cr}$$

where C_{b1} and C_{b2} are the damping values for each of the bearings. The optimum damping ratio can be approximated from the stiffness ratio as:

$$\xi_{opt} = (1 + \bar{K})/2$$

These ratios can be calculated for both the horizontal and vertical directions. However, the gravitational rotor load normally causes the bearing stiffness to be higher in the vertical direction than in the horizontal direction. Thus, the vertical stiffness is usually most important.

Two case studies will be presented in order to demonstrate the application of these bearing design concepts. It should be emphasized that the rules of thumb and design criteria applied here are not universal-design rules that apply in all cases. They are simply guidelines that can assist the designer in the pursuit of the optimum bearing design.

CASE STUDIES

Seven-Stage Centrifugal Compressor

A seven-stage centrifugal compressor, as shown in Figure 14, which had exhibited high vibration in the field, figured in the first case. This was a 1942 lb rotor with a 74.4 in bearing span. The rotor was supported in two, 3.62 in diameter journal bearings. A critical speed map for the compressor showing the first three modes is depicted in Figure 15. Note that the rigid bearing critical was 3685 rpm and the operating speed was 6900 rpm. Also note the flatness of the first mode curve, which is typical of a long, flexible rotor. The stiffness of this shaft is only 3.7×10^5 lb/in.

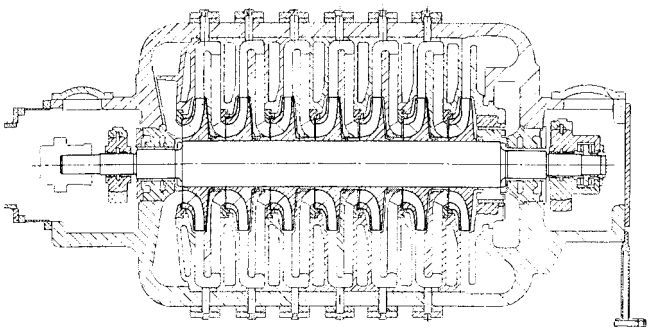

Figure 14. Seven-Stage Centrifugal Compressor.

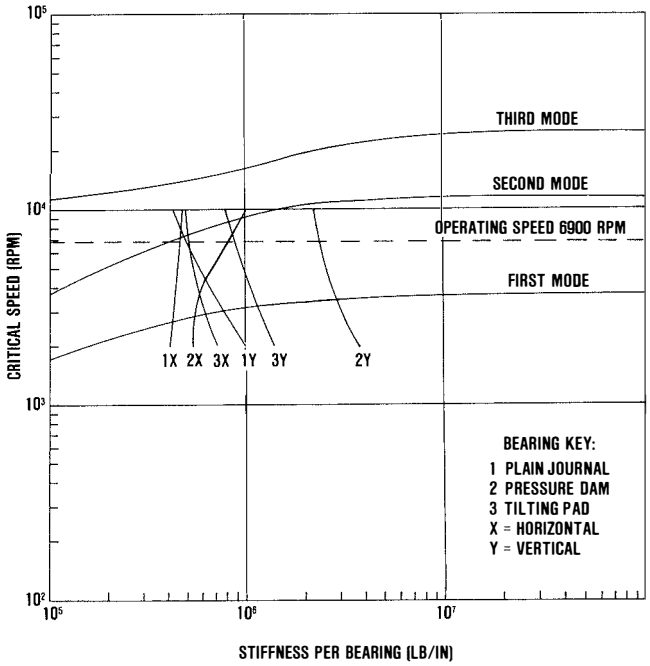

Figure 15. Undamped Critical Speed Map for Seven-Stage Centrifugal Compressor.

The original bearing design, shown in Figure 16, was a double-land plain cylindrical journal bearing, which consisted of a pair of 2.0 in lands. Therefore, the slenderness (L/D) ratio of each land is 0.55. The diametral bearing clearance range was 6.0 to 8.0 mils, which represents 1.6 to 2.2 mils per inch of journal diameter (an 8.0 mil clearance will be assumed in this

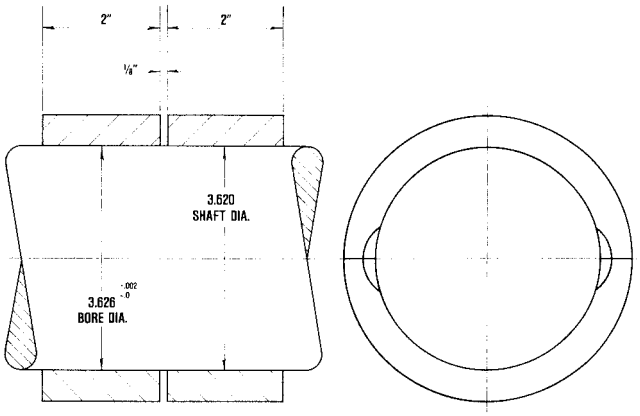

Figure 16. Double-Land Plain Cylindrical Journal Bearing.

case). As shown in Table 1, these bearings had an acceptable stiffness ratio of 3.6, but the logarithmic decrement value of −0.41 indicates that the rotor was unstable. The data measured on the machine confirmed that this instability prediction was correct. In an attempt to increase stability, these bearings were modified to a pressure dam design. A pressure dam and a relief groove were cut into each of the lands as shown in Figure 17. The reason for modifying both lands is not known, but it could have been simply to preserve symmetry. The dam widths were 47.5 percent of each land width, the radial clearance in the dam step was 4.25 times the bearing radial clearance, the dam angle was 130 degrees from the split line, and the relief track widths were 21 percent of each land width. This modification did improve the rotor stability to a marginally

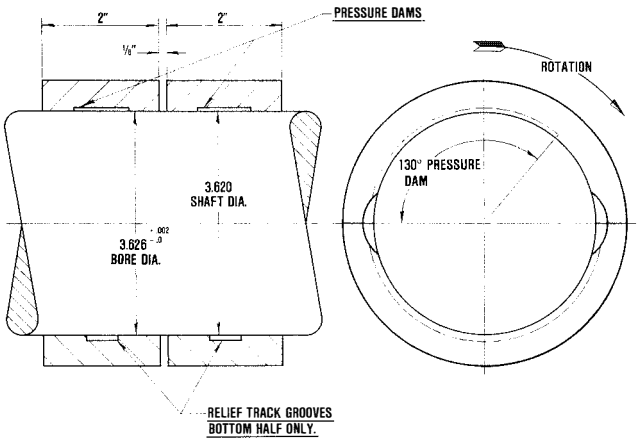

Figure 17. Double-Land Pressure Dam Bearing.

Table 1. Bearing Stiffness and Damping Ratios for Seven-Stage Centrifugal Compressor.

ROTOR WEIGHT, W = 1,942 LB
RIGID BEARING CRITICAL SPEED, N_{Cr} = 3,685 RPM
SHAFT STIFFNESS, $K_S = 3.744 \times 10^5$ LB/IN
CRITICAL DAMPING, C_{Cr} = 1,941 LB-SEC/IN

BEARING TYPE	VERTICAL STIFFNESS RATIO AT N_{Cr}	OPTIMUM DAMPING RATIO	ACTUAL DAMPING RATIO AT N_{Cr}	PERCENT OF OPTIMUM DAMPING	LOG DECREMENT	STABILITY CONDITION
PLAIN JOURNAL	3.6	2.3	4.7	204	-0.41	UNSTABLE
PRESSURE DAM	14.6	7.8	7.0	90	+0.13	MARGINAL
TILT PAD	5.8	3.4	2.7	79	+0.45	STABLE

stable logarithmic decrement value of +0.13. However, the resulting bearing stiffness was too high, as indicated by the stiffness ratio of 14.6 in Table 1. The critical speed map also indicated this problem, because the vertical stiffness was shown to intersect the first mode curve in the rigid bearing region. Therefore, the pressure dam modification was unacceptable.

Based upon the previous discussion, two major objectives needed to be met in considering a design alternative. First, the bearing stiffness had to be reduced to the flexible bearing range and the rotor stability needed improvement. These criteria were met with the five shoe tilting-pad bearing conversion, shown in Figures 18, 19 and 20. The new design had 2.5 in pads, 25 percent preload, 6.0 mil diametral set clearance and load-between-pad orientation. With these redesigned bearings, the stiffness ratio was reduced to 5.8 and the logarithmic decrement was increased to a very stable value of +0.45. The resulting horizontal and vertical stiffness curves for the final tilting-pad bearing design are shown in Figure 15. Since the bearing retrofit, this compressor has been operating successfully in a refinery for several years.

18,000 Horsepower Steam Turbine

A two-stage, 18,000 horsepower steam turbine shown in Figure 21 was the principle figure in case number two [26]. This was a 913 lb rotor, which was operated at 10,300 rpm. Originally, the rotor was supported by two 4.0 in diameter tilting-pad journal bearings, consisting of five rocker-pivot shoes with a length of 1.6 in, preload of 0.0, and load-on-pad orientation.

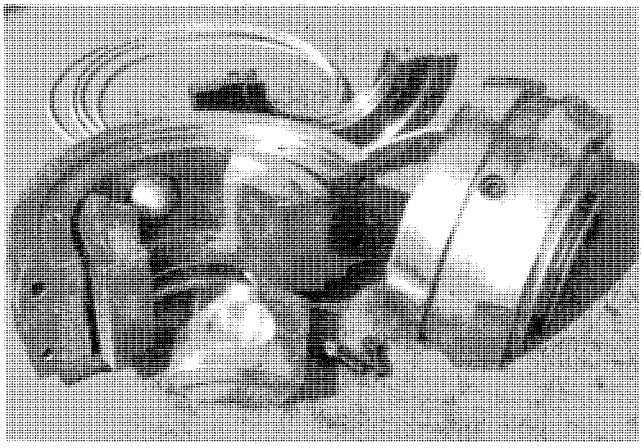

Figure 18. New Tilting-Pad Journal Bearing Hardware for Inlet End of Compressor. Journal Pad Removed to Show Spherical Pivot.

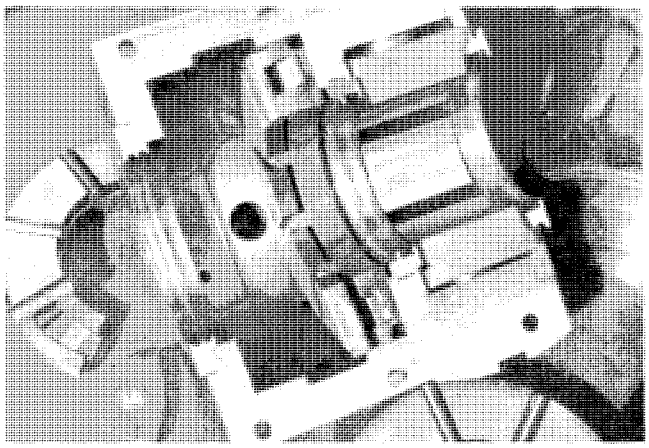

Figure 19. New Tilting-Pad Journal and Thrust Bearing Hardware for Discharge End of Compressor—View into Top Half.

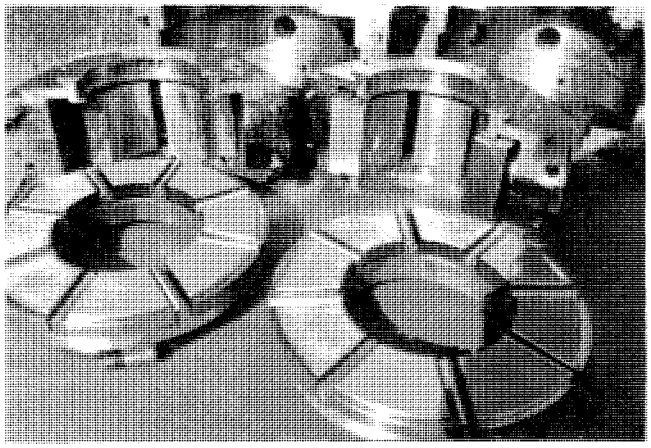

Figure 20. New Journal and Thrust Bearing Hardware for Compressor. Active and inactive thrust bearings, in foreground, show directed lubrication nozzle manifolds between the pads.

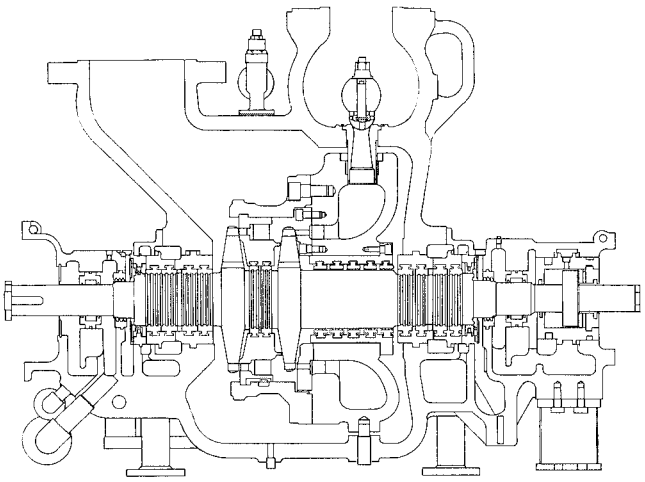

Figure 21. 18,000 HP Steam Turbine.

In the plant, this rotor had exhibited synchronous vibration amplitudes as high as 5.0 mils at the bearings. This level of vibration is unacceptable; particularly when a typical 4.0 in bearing has a diametral operating clearance of only 6.0 to 8.0 mils. These high vibration amplitudes yielded noticable distress in the bearing babbitt lining. This babbitt fatigue failure is illustrated in Figures 22 and 23. One of the bearings showed babbitt fatigue in four out of five pads. The fatigue toward one end of the bearing in Figure 23 indicated a possible misalignment condition.

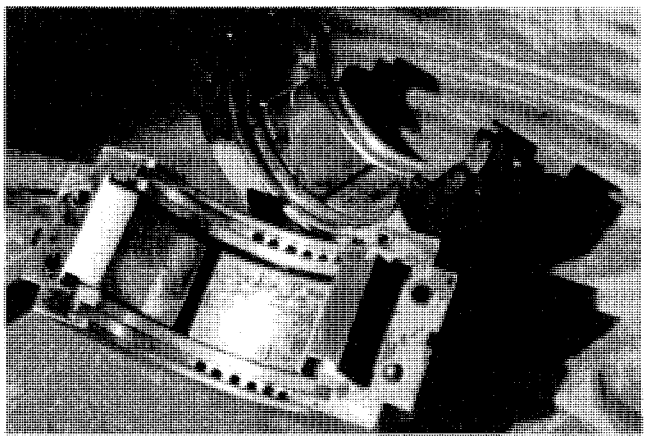

Figure 22. Original Tilting-Pad Journal Bearing for Turbine. Pads have babbitt fatigue damage.

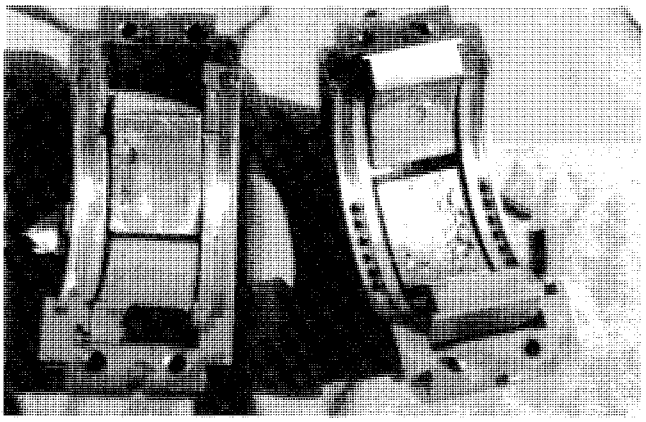

Figure 23. Original Tilting-Pad Journal Bearing. Note babbitt fatigue damage toward one end of bearing, which indicates misalignment.

An undamped critical speed map showing the horizontal and vertical stiffnesses for the original tilting-pad journal bearings, assuming a diametral running (set) clearance of 7.0 mils is shown in Figure 24. The figure shows that the horizontal stiffness line intersects the third mode curve at the running speed. Therefore, the undamped critical speed map indicated a potential critical speed problem. In addition to these problems, there was suspicion of bearing shell looseness due to thermal case distortions.

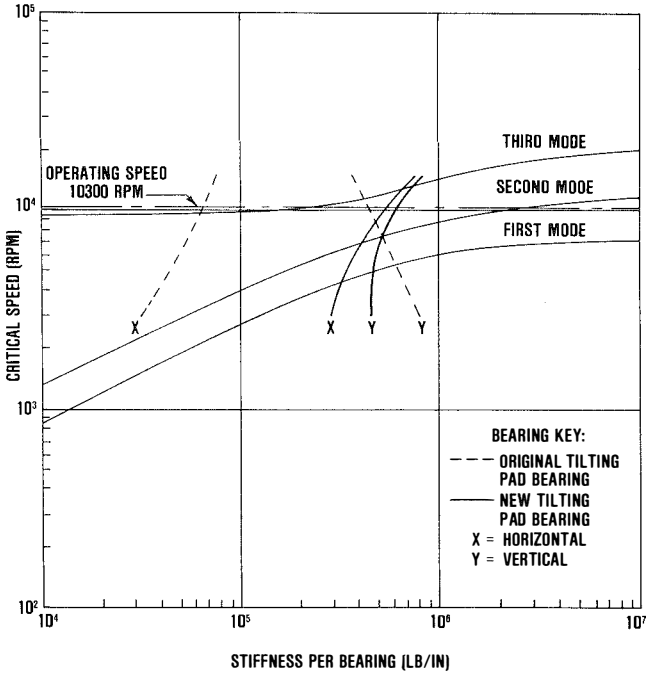

Figure 24. Undamped Critical Speed Map for Two-Stage Steam Turbine Showing Original and New Bearing Stiffnesses.

In order to illustrate the different characteristics that can be obtained for various bearing geometries, the turbine critical speed map containing superpositions of the vertical principal stiffness curves for eight different bearing designs is presented in Figure 25. These eight bearings were selected only for illustration purposes. Numerous geometric combinations are possible for each bearing type. This illustration emphasizes the importance of rotor dynamics optimization techniques as a basis for selecting the best bearing design from the large realm of possibilities. All of the bearings referred to in Figure 25 have 4.0 in journal diameters, slenderness ratios (L/D) of 1.0, and diametral running clearances of 0.006 inches. The lubricant light turbine oil was ISO 32 and the bearing load was 450 lb.

The plain and axial groove bearings are self explanatory. The pressure dam bearing has a radial clearance in the dam step that is 3.0 times the radial bearing clearance [8]; the dam width is 80 percent of the bearing width; the dam angle is 135 degrees from the split line; and there is no relief groove in the bottom half. The lemon bore bearing has a 50 percent preload and the offset bearing has a 50 percent offset. The tilting-pad bearing has five shoes, 80 percent preload, and load-between-pad orientation.

The final bearing design hardware is shown in Figure 26 and 27. The new design is also a five pad, tilting-pad bearing, but the pad length is increased by 56 percent, the preload is

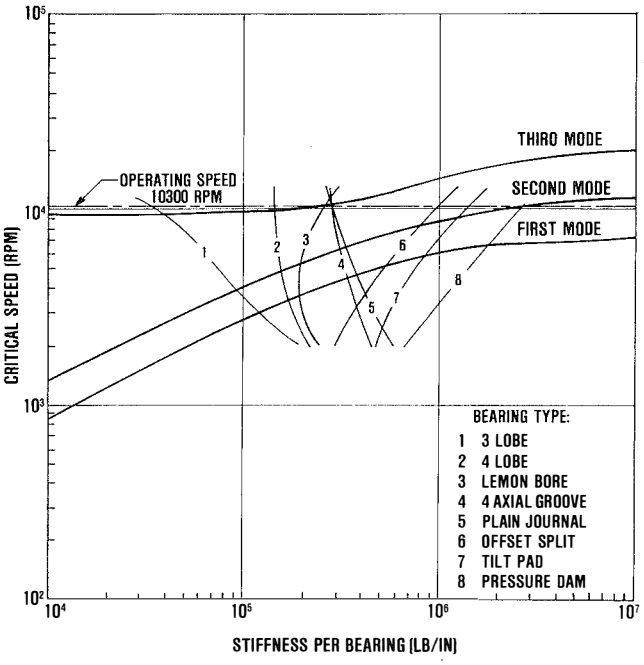

Figure 25. Undamped Critical Speed Map of Two-Stage Turbine Showing Comparison of Stiffnesses for Different Bearing Designs.

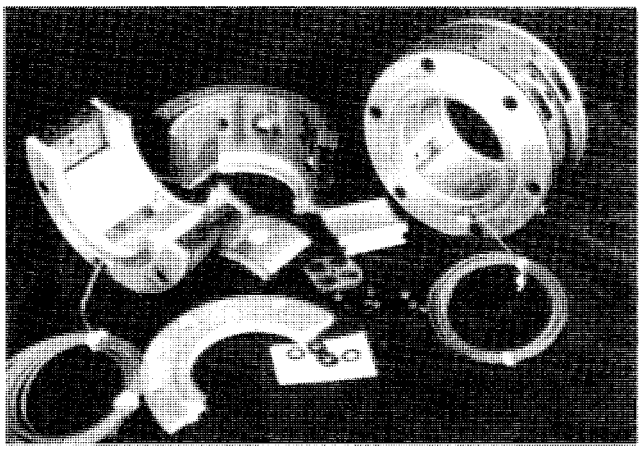

Figure 26. New Tilting-Pad Journal Bearing Hardware for Turbine. Journal pad is removed to show spherical pivot.

increased by 50 percent and orientation is changed to load-between-pads. The new bearing oil film stiffness in both directions was greater as the rotor speed increased, as indicated in Figure 24. Therefore, the third undamped critical speed was raised, because the bearing stiffness curves were shifted relative to the third mode curve of the rotor. A comparison of the stiffness and damping ratios for the original and new bearing designs is presented in Table 2. Note that the original and new designs have the same vertical stiffness and damping ratios at the first rigid critical speed, even though the new design is much stiffer at higher speeds. These new design characteristics were obtained simply by changing the geometric parameters of the tilting-pad bearing.

The spherical pivots behind the pads of the new bearing are shown in Figure 26. This pivot arrangement helped accommodate misalignment. The new design also included integral spring-loaded pads on the outside of the bearing shell, as shown in Figure 27. These pads self-adjust to hold the shell tight within the case. Since the bearing retrofit, the measured vibration at the bearings is less than 1.0 mil.

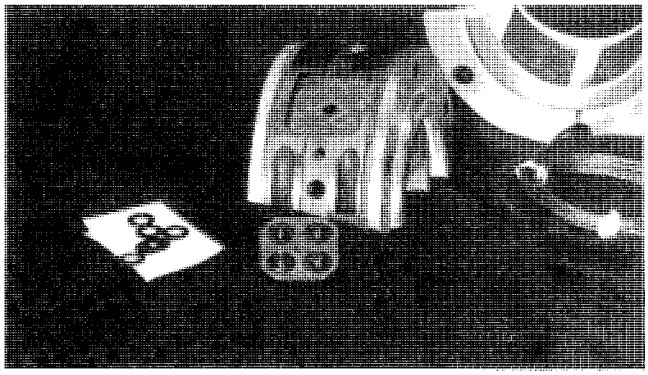

Figure 27. New Bearing Hardware for Turbine. Spring-loaded pad is removed from outside of shell to show belleville spring arrangement.

Table 2. Bearing Stiffness and Damping Ratios for Two-Stage Steam Turbine.

ROTOR WEIGHT, W = 913 LB
RIGID BEARING CRITICAL SPEED, N_{cr} = 7,200 RPM
SHAFT STIFFNESS, $K_S = 6.71 \times 10^5$ LB/IN
CRITICAL DAMPING, C_{cr} = 1,779 LB-SEC/IN

BEARING	VERTICAL STIFFNESS RATIO AT N_{cr}	OPTIMUM DAMPING RATIO	ACTUAL DAMPING RATIO AT N_{cr}	PERCENT OF OPTIMUM DAMPING
(1) ORIGINAL TILT PAD	1.6	1.3	0.9	69
(2) NEW TILT PAD	1.6	1.3	0.9	69

GEOMETRIES: BRG (1) L/D = 0.4, PRELOAD = 0.0, Cset = 0.007, LOAD-ON-PAD
BRG (2) L/D = 0.6, PRELOAD = 0.5, Cset = 0.006, LOAD-BETWEEN-PAD

SUMMARY

A review of a number of hydrodynamic bearing types and two case studies were presented to illustrate bearing applications to industrial turbomachinery. The conclusions reached in these case studies, regarding preference of one bearing type over another, should not be overly generalized. For example, in case number one, the modification of the plain bearing to a pressure dam bearing was an unacceptable alternative for this particular machine. It is important to note that the addition of a pressure dam to a plain journal bearing design has been an economical cure for many bearing instability problems in the past. However, the pressure dam and relief groove can significantly affect the stiffness and damping of the bearing, especially for a double-land bearing. In this case, the modification increased the total bearing vertical stiffness and damping, near the first critical speed by 302 percent and 50 percent, respectively.

In case number two, the original bearings were the tilting-pad type. This retrofit did not require changing the bearing design type. Instead, the new design required a tilting-pad

bearing with longer pads, larger preload and load-between-pad orientation. This geometry change produced the same fluid film vertical characteristics near the first critical speed. However, at other speeds, these characteristics were significantly different. In particular, the increasing bearing stiffness characteristic at elevated speeds raised the third critical speed.

The case studies illustrate the effectiveness of the critical speed map and the stiffness and damping ratios as toools that can assist a designer in preliminary bearing selection. However, these basic tools are only approximate and they should not be substituted for the more complete unbalance response [27,28] and damped stability analyses [29,30,31].

REFERENCES

1. Allaire, P. E. and Flack, R. D., "Design of Journal Bearings for Rotating Machinery," *Proceedings of the Tenth Turbomachinery Symposium*, Turbomachinery Laboratories, Texas A&M University, College Station, Texas, pp. 25-45 (1981).
2. Abramovitz, S., "Fluid Film Bearings Fundamentals and Design Criteria and Pitfalls," *Proceedings of the Sixth Turbomachinery Symposium*, Gas Turbine Laboratories, Texas A&M University (1977).
3. Raimondi, A. A. and Boyd, J., "A Solution for the Finite Journal Bearing and Its Application to Analysis and Design: I, II, III," ASLE (1957).
4. Lund, J. W., "Rotor-Bearing Design Technology; Part III: Design Handbook for Fluid-Film Bearings," Mechanical Technology Incorporated, Technical Report No. AFAPL-TR-65-45 (1965).
5. Rippel, H. C., "Cast Bronze Bearing Design Manual," Cast Bronze Bearing Institute, Inc. (1971).
6. Eierman, R. G., "Stability Analysis and Transient Motion of Axial Groove, Multilobe and Tilting Pad Bearings," M.S. Thesis, University of Virginia (1976).
7. Adams, M. L., "Axial-Groove Journal Bearings," *Machine Design*, pp. 120-123 (April 1970).
8. Nicholas, J. C. and Allaire, P. E., "Analysis of Step Journal Bearings—Finite Length, Stability," Trans. ASLE *23*(2), pp. 197-207 (1980).
9. Nicholas, J. C., Allaire, P. E. and Lewis, D. W., "Stiffness and Damping Coefficients for Finite Length Step Journal Bearings," Trans. ASLE, *23*(4), pp. 353-362 (1980).
10. Allaire, P. E., Nicholas, J. C. and Barrett, L. E., "Analysis of Step Journal Bearings—Infinite Length, Inertia Effects," Trans. ASLE, *22*(4), pp. 333-341 (1979).
11. Lund, J. W. and Thomsen, K. K., "A Calculation Method and Data for the Dynamic Coefficients of Oil-Lubricated Journal Bearings," *Topics in Fluid Film Bearings and Rotor Bearing System Design and Optimization*, ASME Book No. 100118, pp. 1-28 (1978).
12. Kirk, R. G., "The Influence of Manufacturing Tolerance on Multi-Lobe Bearing Performance in Turbomachinery," *Topics in Fluid Film Bearing and Rotor Bearing System Design and Optimization*, ASME Book No. 100118, pp. 108-129 (1978).
13. Falkenhagen, G. L., Gunter, E. J. and Schuller, F. T., "Stability and Transient Motion of a Vertical Three-Lobe Bearing System," Journal of Engineering for Industry, Trans. ASME, Series B, *94*(2), pp. 665-677 (1972).
14. Falkenhagen, G. L., "Stability and Transient Motion of a Hydrodynamic Horizontal Three-Lobe Bearing System," The Shock and Vibration Digest, *7*(5) (1975).
15. Lund, J. W., "Rotor-Bearing Dynamics Design Technology, Part VII: The Three-Lobe Bearing and Floating Ring Bearing," Mechanical Technology Incorporated, Technical Report No. AFAPL-TR-64-45 (1968).
16. Pinkus, O., "Analysis and Characteristics of the Three-Lobe Bearing," Journal of Basic Engineering, Trans. ASME, pp. 49-55 (1959).
17. Lund, J. W., "Spring and Damping Coefficients for the Tilting-Pad Journal Bearing," Trans. ASLE, *7*(4), pp. 342-352 (1964).
18. Nicholas, J. C., Gunter, E. J. and Allaire, P. E., "Stiffness and Damping Coefficients for the Five Pad Tilting Pad Bearing," Trans. ASLE, *22*(2), pp. 113-124 (1979).
19. Shapiro, W. and Colsher, R., "Dynamic Characteristics of Fluid-Film Bearings," *Proceedings of the Sixth Turbomachinery Symposium*, Gas Turbine Laboratories, Texas A&M University, College Station, Texas (1977).
20. Jones, G. J. and Martin, F. A., "Geometry Effects in Tilting-Pad Journal Bearings," ASLE Preprint No. 78-AM-2A-2 (1978).
21. Ettles, C. M. McC., "The Analysis and Performance of Pivoted Pad Journal Bearings Considering Thermal and Elastic Effects," Journal of Lubrication Technology, Trans. ASME, ASME Paper No. 79-LUB-31 (1979).
22. Abdul-Wahed, M. N., Frene, J. and Nicolas, D., "Analysis of Fitted Partial Arc and Tilting-Pad Journal Bearings," ASLE Preprint No. 78-AM-2A-3 (1978).
23. Raimondi, A. A. and Boyd, J., "An Analysis of the Pivoted-Pad Journal Bearing," Mechanical Engineering, pp. 380-386 (1953).
24. Barrett, L. E., Gunter, E. J. and Allaire, P. E., "Optimum Bearing and Support Damping for Unbalance Response and Stability of Rotating Machinery," Journal of Engineering for Power, Trans. ASME, *100*(1), pp. 89-94 (1978).
25. Jeffcott, H. H., "The Lateral Vibration of Loaded Shafts in the Neighborhood of a Whirling Speed—The Effect of Want of Balance," Phil. Mag., Series 6, *37*, p. 304 (1919).
26. Salamone, D. J., "Bearing Replacements for Turbomachinery," *Vibration Institute Proceedings—Machinery, Vibration, Monitoring and Analysis*, pp. 57-60 (April 1981).
27. Lund, J. W. and Orcutt, F. K., "Calculations and Experiments on the Unbalance Response of a Flexible Rotor," Journal of Engineering for Industry, Trans. ASME, Series B, *89*(4), pp. 785-796 (1967).
28. Salamone, D. J. and Gunter, E. J., "Effects of Shaft Warp and Disk Skew on the Synchronous Unbalance Response of a Multimass Flexible Rotor in Fluid Film Bearings," *Topics in Fluid Film Bearing and Rotor Bearing System Design and Optimization*, ASME Book No. 100118 (1978).
29. Gunter, E. J., "Dynamic Stability of Rotor-Bearing Systems," NASA SP-113, Office of Technical Utilization, U.S. Government Printing Office, Washington D.C. (1966).
30. Lund, J. W., "Stability and Damped Critical Speeds of a Flexible Rotor in Fluid Bearings," Journal of Engineering for Industry, Trans. ASME, Series B, *96*:2, pp. 509-517 (1974).

31. Gunter, E. J. and Trumpler, P. R., "The Influence of Internal Friction on the Stability of High Speed Rotors with Anisotropic Supports," Journal of Engineering for Industry, Trans. ASME, Series B, *91*:4, pp. 1105-1128 (1969).

BIBLIOGRAPHY

Fuller, D. D., *Theory and Practice of Lubrication for Engineers*, New York: John Wiley and Sons, Inc. (1956).

Gross, G. A., *Fluid Film Lubrication*, John Wiley and Sons, Inc. (1980).

Martin, F. A. and Garner, D. R., "Plain Journal Bearings Under Steady Loads: Design Guidance for Safe Operation," First European Tribology Congress, I MECH E, Paper No. C313/73 (1974).

Wilcock, D. F. and Booser, R. E., *Bearing Design and Application*, New York: McGraw-Hill, (1957).

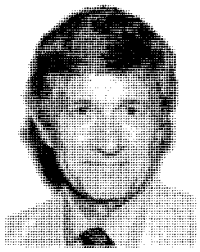

Bernard S. Herbage is President and Technical Director of Centritech Corporation. He is a registered professional engineer in the State of Texas. He received his B.S.M.E. degree from Bradley University where he was also a member of the honorary fraternity of engineers, Tau Sigma.

The first ten years of Mr. Herbage's engineering career were spent with Allis-Chalmers—nine years of which were in the Mechanical Design Section of the Steam Turbine and Large Generator Departments, and then one year as Supervisory Engineer in the Research Division developing new products. During this period Mr. Herbage concentrated a considerable amount of his time in the design, application, and testing of high capacity thrust and journal bearings.

After his Allis-Chalmers experience, he continued to pursue his interest in Fluid Film Bearings by moving to Waukesha Bearings Corporation, working in various positions as Chief Engineer, General Manager, and Vice-President. There he worked with virtually every major high speed rotating machinery manufacturer in the design and application of fluid film thrust and journal bearings.

Centritech Corporation, founded in 1971, is a highly successful, growth orientated company specializing in the design and manufacture of fluid film bearings, fluid film seals, and labyrinth seals, with emphasis on end-user problem solving of turbomachinery, often requiring the application of in-house rotor dynamic capability.